

1 **In Silico Analysis of Drug Off-Target Effects on Diverse Isoforms of Cervical**
2 **Cancer for Enhanced Therapeutic Strategies**

3 Azhar Iqbal¹, Faisal Ali¹, Moawaz Aziz¹, Asad Ullah Shakil¹, Shanza Choudhary¹, Adiba
4 Qayyum¹, Fiza Arshad¹, Sarah Ashraf¹, Sheikh Arslan Sehgal², Momina Hussain¹, Muhammad
5 Sajid¹

6 ¹Department of Biotechnology, University of Okara, Okara, Punjab, Pakistan

7 ²Department of Bioinformatics, Islamia University Bahawalpur, Bahawalpur, Punjab, Pakistan

8

9 Corresponding Author:

10 Muhammad Sajid¹

11 Green Town Renala Khurd, Renala Khurd, Punjab, 56300, Pakistan

12 Email address: infobiotec@uo.edu.pk

13

14

15

16

17

18

19

20

21

22

23

24
25
26
27
28
29
30
31
32
33
34
35
36
37
38
39
40
41
42
43
44
45
46
47
48
49
50
51

Abstract

Cervical cancer is a severe medical issue as 500,000 new cases of cervical cancer are identified in the world every year. The selection and analysis of the suitable gene target are the most crucial in the early phases of drug design. The emphasis at one protein while ignoring its several isoforms or splice variations may have unexpected therapeutic or harmful side effects. In this work, we provide a computational analysis of interactions between cervical cancer drugs and their targets that are influenced by alternative splicing. By using open-accessible databases, we targeted 45 FDA-approved cervical cancer drugs targeting various genes having more than two distinct protein-coding isoforms. Binding pocket interactions revealed that many drugs do not have possible targets at the isoform level. In terms of size, shape, electrostatic characteristics, and structural analysis have shown that various isoforms of the same gene with distinct ligand-binding pocket configurations. Our results emphasized the risks of ignoring possibly significant interactions at the isoform level by concentrating just on the canonical isoform and promoting consideration of the impacts of cervical cancer drugs on- and off-target at the isoform level to further research.

Keywords

Cervical Cancer, Isoforms, Molecular docking, Interaction analysis, Bioinformatics approaches

52

53

54 **1. Introduction**

55 In developing countries, cervical cancer is the main reason for cancer-related deaths and years of
56 life loss (1). Several years earlier than the median age at which breast, lung, and ovarian cancers
57 are diagnosed, cervical cancer is commonly diagnosed in one's fifth decade of life (2). Ninety
58 percent of the 270 000 cervical cancer fatalities in 2015 happened in low- and middle-income
59 countries (LMIC), where mortality is 18 times higher than in developed nations (3). Nearly all
60 cervical cancers are caused by high-risk subtypes of the human papillomavirus (HPV), whereas
61 screening and vaccination programs are effective disease preventive measures for HPV (4). The
62 two most prevalent histological subtypes (squamous cell carcinoma, and adenocarcinoma)
63 account for 70% and 25% of all cervical malignancies, respectively (5, 6). The major decrease in
64 cervical cancer mortality has been attributed to the development and implementation of
65 screening programs (7). Cervical cancer has a poor prognosis following metastasis or recurrence;
66 the 5-year overall survival (OS) rate is about 17% (8). In order to improve the treatment efficacy
67 of cervical cancer, it is crucial to uncover novel therapeutic targets and survival-associated
68 biomarkers.

69 Major innovations in large-scale multi-omics research provide a unique perspective for the
70 systems biology analysis of the emergence and spread of cancer. HPV contributes to the
71 development of cervical cancer, which is considered a virus-driven malignancy. Early HPV
72 infection may simply be a result of external causes, like changes in the genome would eventually
73 cause cervical epithelial cells to convert into malignant (for example, gene fusion, non-coding
74 RNAs, copy number variation, DNA methylation, and somatic DNA mutations) (9-13).
75 Transcriptome and epigenetic modifications have been the focus of the bulk of previous
76 prospective studies. However, Alternative splicing (AS) in cancer post-transcriptional isoforms
77 hasn't been thoroughly studied yet.

78 In eukaryotes, a remarkable biological process known as alternative splicing, which promotes
79 proteome diversity, allows a single gene to express several protein isomers. In humans, where
80 more than 94% of genes are alternatively spliced, the occurrence and properties of alternative

81 splicing are also highly diverse (14-16). This method enables cancer cells to generate abnormal
82 proteins with altered functional domains that promote carcinogenesis (17-19). In malignancies,
83 these domain changes can lead to complicated remodeling and protein-protein interactions. Some
84 essential oncogenic splicing variations have the ability to control tumor epithelial-to-
85 mesenchymal transition and biological processes of cancer stem cell (20). Gene expression is
86 properly controlled to occur in a context-specific way, even if gene isoforms commonly appear
87 to have different, sometimes even opposing functions.

88 Aberrant isoforms, or spliced variations that cause disease, have the potential to be effective drug
89 targets in addition to serve as significant biomarkers (21, 22). In this study, we primarily focused
90 on cervical cancer and examined whether or not the drugs are effective against the target gene
91 isoforms. In this work, we examined the effectiveness of FDA-approved drugs against the
92 various isoforms of the cervical cancer-related genes. Using structural analysis and the clinical
93 data on the expression of these genes, we curated the drug interaction data for the various
94 isoforms of different genes implicated in cervical cancer and evaluated their effectiveness against
95 isoforms.

96

97

98

99

100

101

102

103

104

105

106

107

108

109

110

111

112

113 **2. Methods**

114 **2.1 Collection of genes and their isoforms**

115 We found the genes associated with cervical cancer using COSMIC database (23) which is an
116 online resource of somatically acquired mutations reported in human cancer. There are more than
117 30 genes that may contribute to cervical cancer shown in Supplementary File 1. Based on the
118 number of patient samples, the top 5 genes out of 30 were selected, and these genes were then
119 used for further analysis. The Ensemble genome database (24) was used to curate the isoforms
120 and protein sequences for these genes. Using COSMIC Mutation ID, the mutations were
121 identified in genes and matched with the variants of each isoform using the Ensemble database.

122 **2.2 Curation of drugs-target interaction data**

123 By using the Drug Gene Interaction Database (DGIdb) (25), we curated the FDA Approved
124 drugs for our genes. Through this database, more than 40 drugs that have received FDA approval
125 were found. These drugs were retrieved from the Drug Bank (26) and chEMBL (27).

126 **2.3 Sequence analysis of isoforms**

127 To check the conservation of binding pocket in isoforms of the genes, Binding Pockets of the
128 canonical proteins were predicted through the COACH Server (<https://zhanggroup.org/COACH/>
129). We found domains from EMBL-EBI InterPro database (28) and aligned these with the
130 sequences of the canonical protein and their isoforms. Using the Bioconductor programme msa,
131 which offers a selection of alignment techniques and produces alignment plots in LaTeX format ,
132 we created numerous alignments of sequences. Using the Cluster Omega method included in the
133 msa package, we created an alignment of the binding site sequence with all of the protein
134 isoforms of the same gene.

135 **2.4 Isoforms expression in normal and tumors samples**

136 We looked at the clinical data offered by UCSC Xena (29) for cervical cancer patients which is
137 an online resource for analyzing multi-omics, clinical, and phenotypic data. We used UCSC
138 Xena to compare TCGA tumor samples to GTEx normal samples to evaluate whether protein
139 coding isoforms are up- or down-regulated in cervical cancer. The expression of protein isoforms
140 was examined in patient normal samples using GTEx and tumor samples using TCGA, both of
141 which were drawn from the 307 Cervical Cancer Samples that are available in the UCSC Xena
142 database. We also visualized the exon structure of the isoforms to better understand the pattern of
143 alternative splicing in the various isoforms of the genes.

144 **2.5 Structure Prediction of Protein Isoforms and Ligand Docking**

145 To better understand the associations between the proteins with their ligands (drugs), we
146 predicted the 3D structures of protein isoforms using a number of tools for structural level study
147 of the different isoforms of the proteins. Protein isoform structures were predicted through the
148 use of the structure prediction tools trRosetta (30) , Robetta (31), Swiss-Model (32) , and I-
149 TASSER (33). Further, the ERRAT quality factor and the favored region, allowed region, and
150 disabled region in the Ramachandran plot were used to evaluate the predicted structures.
151 After evaluating, We utilized SiteMap53 (34) to determine the drug targets region in those
152 protein isoforms' 3D structures. Through the use of Chimera 1.15rc, predicted 3D structures for
153 the isoforms were further prepared for docking analysis. We used Pyrex software to investigate
154 the ligand-protein docking analysis, and we took into account a number of drugs that have
155 already been approved for such proteins so that we can check these drugs' effectiveness against
156 various protein isoforms that are affected by disease. Poses of the Protein-Ligand Complexes
157 were captured for further analyzing the pocket sizes, shapes, and electrostatic surfaces of docked
158 protein isoforms.

159 **2.6 Interaction analysis**

160 The Discovery Studio 2021 Client was used to examine protein-ligand complexes. We examined
161 that how the drug, which has a high binding affinity value with the canonical protein, interacts
162 with the different isoforms. Further, we examined the interactions between hydrophobic and
163 hydrogen sites in different docked protein isoforms

164 3. Results

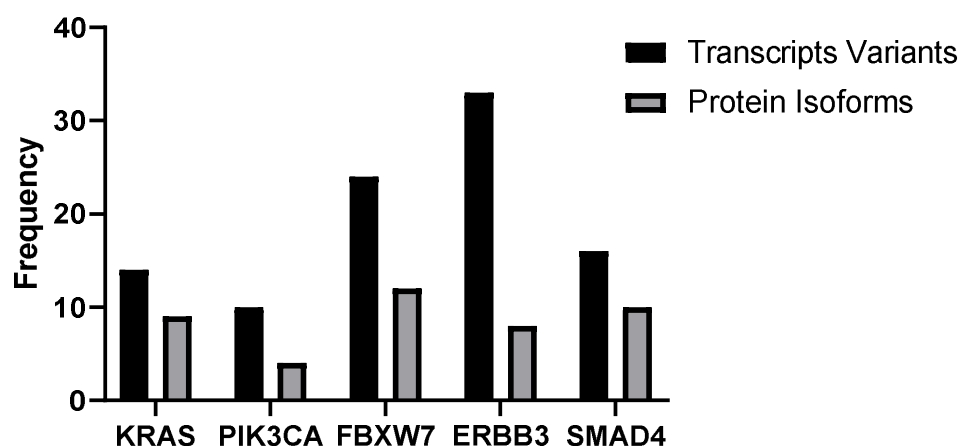
165 3.1 Drugs Target Genes have multiple Isoforms

166 More than 30 genes linked to cervical cancer were identified to have missense mutations show in
167 Supplementary File 1. Keeping in view the number of the patient samples, we chose five genes
168 for further analysis. We found FDA-approved drugs interactions to analyze the interactions
169 among drug and its target protein isoforms. We were able to retrieve more than 145 entries
170 belonging to 5 distinct genes of Cervical Cancer.

171 **Table 1.** FDA Approved Drugs against target genes and number of protein-coding isoforms.

Genes	FDA Approved Drugs	Number of Transcript	Number of Isoforms
KRAS	Cetuximab, AZD-4785, Selumetinib, CC-223, AZD-8835, PD-0325901, Trametinib, Ridaforolimus	14	9
SMAD4	Lysine, Sapanisertib, Fluorouracil, Alectinib, Crizotinib, Cetuximab, Gemcitabine, Irionotecan, Carboplatin, Paclitaxel	10	4
PIK3CA	Trastuzumab, Temsirolimus, Serabelisib, Taselisib, CC-223, INK-1117, Alpelisib, Buparlisib, Capiwasertib	16	10
ERBB3	Pertuzumab, Trastuzumab, MM-121, AV-203, AMG-888, Patritumab, Duligotuzumab, Sapitinib, MM-111	33	12
FBXW7	Temsirolimus, Sirolimus, Regorafenib, Vorinostat, Belinostat, Entinostat, Docetaxel, Vorinostat, AR-42	24	8

172
173 A partial list from a summary table is shown in Table 1. We identified the bulk of the candidate
174 genes had two or even more transcribed spliced variants and protein isoforms Fig. 1.



175
 176 **Fig. 1** Shows the number of transcript variants and the protein coding isoforms of canonical
 177 proteins.

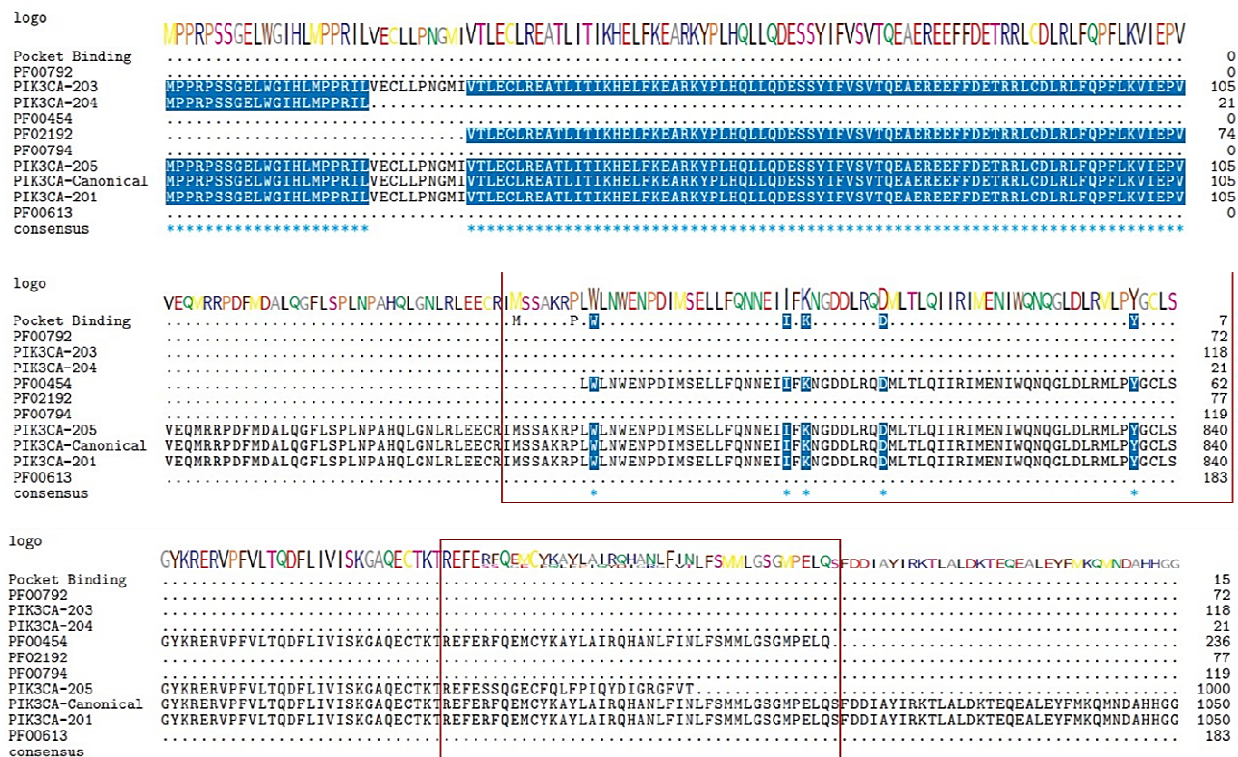
178 Our findings demonstrate that the majority of cancer drug target genes undergo splicing and
 179 make many protein isoforms which may be functionally distinct and react with drugs in different
 180 manner, highlighting the significance of getting isoforms and alternative splicing into account in
 181 drug development.

182 **3.2 Protein isoforms shows differences in the binding pockets**

183 Using several sequence alignments, we were able to pinpoint the precise interaction residues in
 184 each isoform's drug binding region. We carried out multiple sequence alignment between the
 185 Pfam functional domains, the canonical protein, isoform sequences, and the predicted protein
 186 binding pocket. Here we describe some sequence alignment plots of few genes.

187 Cellular functions essential for the development of cancer, such as cell growth, proliferation,
 188 motility, survival, and metabolism, are regulated by the PI3KCA protein (35). PIK3CA gene has
 189 4 isoforms (PIK3CA-201, PIK3CA-203, PIK3CA-204 and PIK3CA-205). Isoforms PIK3CA-
 190 203 & 204 have 21 and 118 residues respectively which completely lacks the predicted pocket
 191 binding Fig. 2. Canonical Protein and Isoforms PIK3CA-201 & 205 found to have identical
 192 sequences in the predicted binding pocket. However, we found variations in the C-terminal
 193 regions and domain PF00454 of isoforms PIK3CA-201 & 205 Fig. 2. We examined the C
 194 terminal region of the Canonical protein, PIK3CA-201 & 205, and Pfam domain PF00454 to

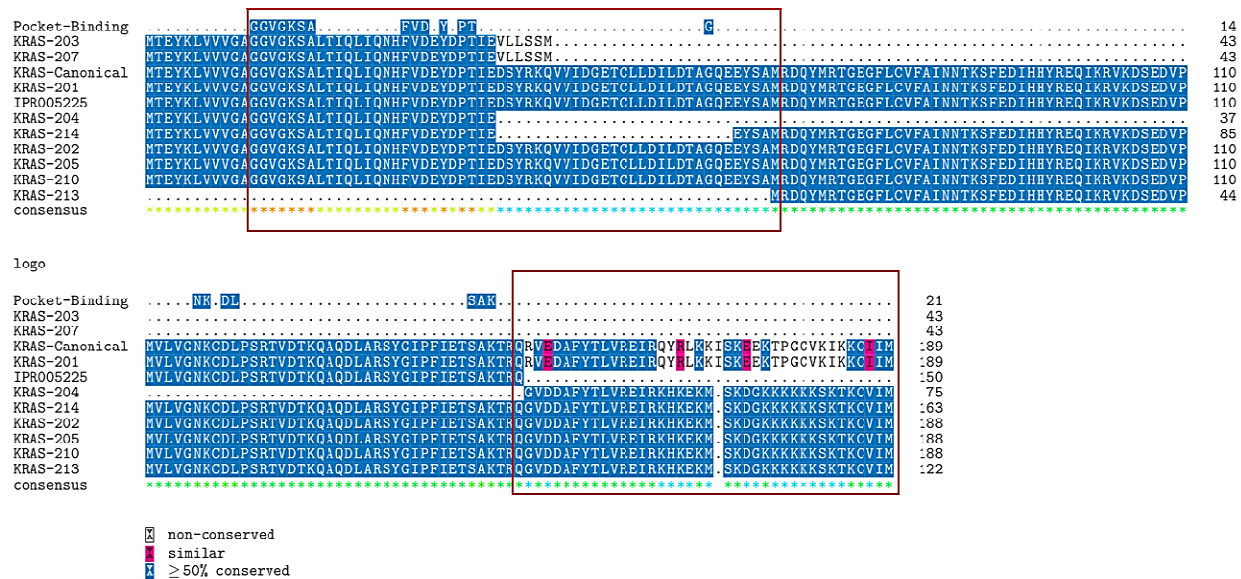
195 further explain this variation. Through the previous studies we found that the C terminal region is
 196 necessary for catalysis. In the absence of membrane, it reduces the enzyme's baseline activity
 197 while promoting membrane binding. This has been suggested to be a crucial PI3Ks regulating
 198 component (36). And the Pfam domain is one of the domains of p100 α catalytic subunit of the
 199 PIK3CA. However, in USP13-PIK3CA, the whole C-terminal region is replaced with the
 200 USP13 protein, which affects catalysis. Since PIK3CA-201 and PIK3CA-205 have the same
 201 upstream regions overall, the fusion proteins produced by the two isoforms should ideally have
 202 the same structure. Additionally, we aligned two other USP13-PIK3CA protein sequences in the
 203 FusionGDB database to support this claim, and all sequences have overlapping interference
 204 residues with the predicted pocket binding Supplementary File 2. This sequence-level data
 205 indicates that the drug may target all of the USP13-PIK3CA fusion protein's splice-variant
 206 isoforms; as a result, splice-variation within the PIK3CA gene does not influence the binding to
 207 its targets in isoforms PIK3CA-201 &205 while it may affect the PIK3CA-203 & 204 which
 208 does not have the predicted binding pocket.



209
 210 **Fig. 2** Sequence alignments of the predicted pocket binding residues of several PIK3CA protein
 211 isoforms. Using the Bioconductor software msa, Cluster Omega was used to align the binding

212 residues with the isoform sequences. Predicted binding pocket residues, aligned Pfam domains,
 213 and PIK3CA-201, PIK3CA-203, PIK3CA-204, and PIK3CA-205 are shown from top to bottom.
 214 Each line included the consensus sequences' sequence logo at the top. Residues in a sequence
 215 that coincide with the anticipated binding residues are shown by blue shading. The purple
 216 coloring suggests that this residue is conserved in about 50% of all sequences. Similar amino
 217 acids are shown by pink shading.

218 The KRAS gene has been a key target of cancer treatment discovery for decades since it is the
 219 most often mutated oncogene in human malignancies, notably in tumors of the pancreas, colon,
 220 and lung. However, despite these enormous efforts, cancers with KRAS mutations continue to be
 221 among the hardest to treat, in large part due to the emergence of treatment resistance brought on
 222 by the plasticity of tumor cells and/or the acquisition of additional mutations. According to the
 223 multiple sequence alignment of KRAS isoforms, the isoforms KRAS-203, 204 & 207 lack the
 224 binding pockets and are thus not predicted to be targets of drugs that treat the KRAS protein
 225 shown in Fig. 3. While the isoforms KRAS-201,202, 205, 210 and 214 have the same binding
 226 residues and are thus likely to be targeted by drugs. Further investigation revealed that KRAS-
 227 202,205,203, and 204 have variations with KRAS-201 on the C terminal. Our findings indicate
 228 that further effort is required to specifically target the KRAS isoforms.

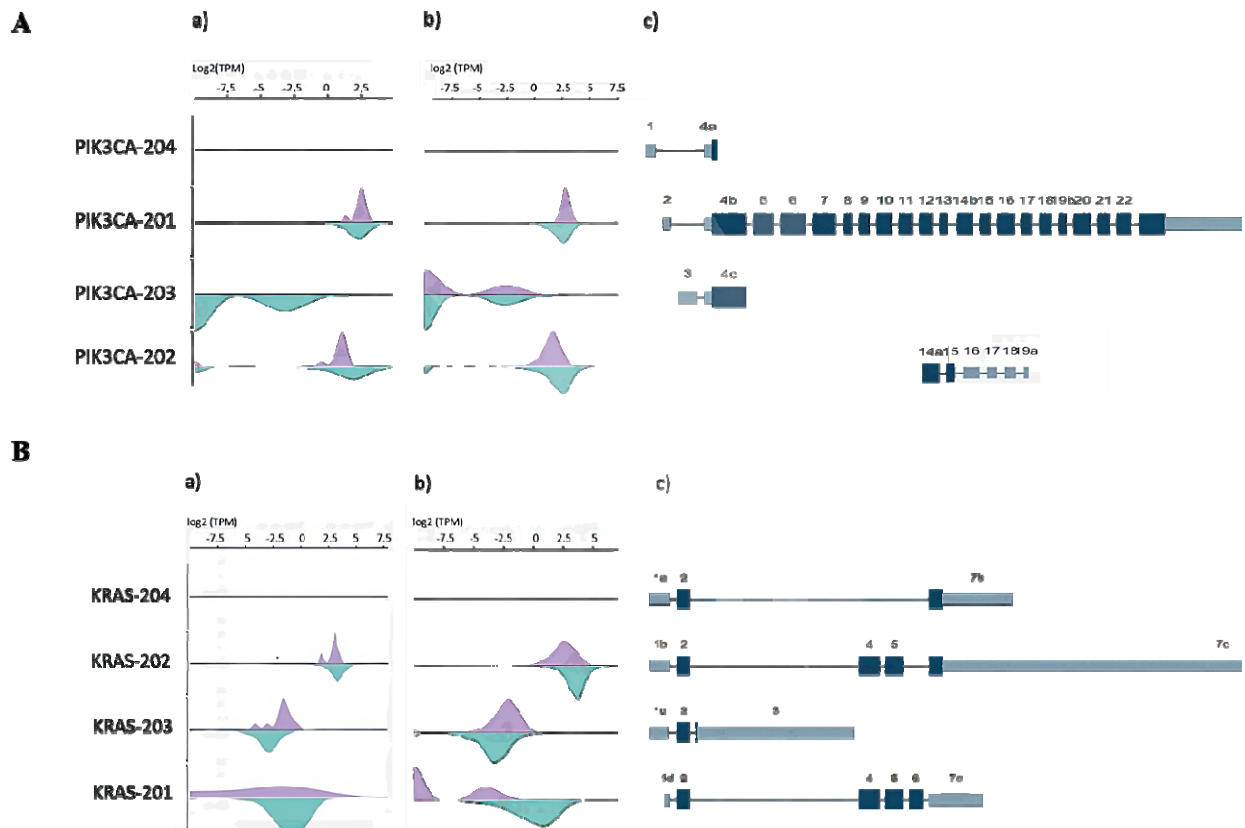


232 residues with the isoform sequences. Predicted binding pocket residues, aligned Pfam domains
233 and KRAS isoforms are shown from top to bottom. Each line included the consensus sequences'
234 sequence logo at the top. Residues in a sequence that coincide with the anticipated binding
235 residues are shown by blue shading. The purple coloring suggests that this residue is conserved
236 in about 50% of all sequences. Similar amino acids are shown by pink shading.

237 **3.3 High Levels of Isoform Expression in Tumor Tissues**

238 Using clinical information from UCSC Xena that is accessible through several projects (TCGA,
239 GTEx and TARGET), we were able to determine the expression of protein isoforms. In TCGA
240 samples of cervical cancer and breast cancer, we observed the expression of PIK3CA and KRAS
241 isoforms shown in Fig. 4A. The expression of isoforms was nearly same in both cancer types.
242 The isoform (PIK3CA-204/ENST00000477735.1) does not express in tumor and normal
243 samples, and is thus ignored. The isoform (PIK3CA-203/ ENST00000468036.1) is highly
244 expressed in the TCGA tumor samples, in contrast to the normal GTEx samples. While we
245 previously found that isoform-203 does not have the predicted binding pocket but we observed
246 that tumor cells express it. Thus, this should be included in future study to examines the on- and
247 off-target effects of drugs.

248 Using transcriptome expression data from the TCGA repository, it was possible to compare the
249 expression of KRAS isoforms (KRAS-202/ENST00000311936.7, KRAS-
250 203/ENST00000556131.1, and KRAS-204/ENST00000557334.5) in cervical and breast samples
251 Fig. 4B. In comparison to normal samples, tumor samples were shown to have higher levels of
252 KRAS-203 expression. Sequence analysis of FBXW7, ERBB3 & SMAD4 are shown in
253 supplementary file 3. Future studies analyzing the on- and off-target effects of drugs should
254 consider these isoforms as these are expressed in tumors



255

256 **Fig. 4 A** PIK3CA isoform expression and exon structure. Green density represents log₂(TPM)
 257 from GTEx normal samples, whereas purple density represents those from a) TCGA Cervical
 258 Cancer samples and b) TCGA Breast Cancer samples. Density plots and c) the exon structure
 259 plot both follow the same sequence. **B** KRAS isoform expression and exon structure. Four
 260 isoforms are related (from top to bottom). Green density represents those from GTEx normal
 261 samples, whereas purple density means a) TCGA Cervical Cancer samples and b) TCGA Breast
 262 Cancer Samples. Density plots and c) the exon structure plot both follow the same sequence.
 263 Every plot is generated using the UCSC Xena browser (37).

264 3.4 Drugs Interaction on Structural Level

265 Even though we have shown changes in binding pockets across isoforms at the sequence level,
 266 structural-level research is the only way to gain more solid proof that the drugs bind to their
 267 targets' isoforms in distinct ways. We have studied the KRAS gene, which has seven distinct
 268 isoforms, together with known drugs that target them in to understand how a certain drug
 269 molecule interacts with several isoforms of a protein.

270 The 3D structures of each isoform were predicted using various databases. The best predicted
271 structures were projected to have ERRAT scores greater than 94. While structures with poor
272 ERRAT values were further improved.

273 Then, using Pyrex, we conducted docking analysis while taking into account a selection of drugs
274 that have been identified to target this disease protein target. After analyzing the docked
275 positions, we observed that although some drugs bind similarly to isoforms, while others bind
276 extremely differently. For instance, Isoforms KRAS-203, 204 & 207 showed low binding
277 affinity with the FDA Approved drugs (Table 2). It supports our previous findings that these
278 isoforms have very small sequences and do not have the predicted binding pocket. While all
279 other isoforms of KRAS (KRAS-201, 202, 205, 210, 213 & 214) have high binding affinities.
280 AZD-4785 had good scores for KRAS-201, 202, 205, and 214. These six isoforms of the protein
281 had strong binding affinity against Trametinib, although KRAS-202 had low binding affinity.
282 With ridoforolimus, all isoforms had the good binding affinities. While the remaining drugs
283 likewise shown good binding affinities with these isoforms, certain isoforms displayed lower
284 affinities than others.

285 **Table 2** Binding Affinity Values of the KRAS-Canonical protein and its isoforms.

Drugs	KRAS-Canonical	KRAS-201	KRAS-202	KRAS-205	KRAS-214	KRAS-213	KRAS-210	KRAS-203	KRAS-204
AZD-4785	-6.9	-7.3	-7.2	-7	-7.2	-6.4	-7.9	-5.7	-4
AZD-8835	-8.3	-8.2	-8.2	-8.7	-7.9	-7.7	-8.5	-6.3	-4.9
CC-223	-7.2	-7.7	-7.5	-7.5	-7.7	-7.3	-7.7	-6.1	-4.5
PD-0325901	-7.7	-7.3	-6.9	-6.9	-7.4	-6.3	-6.8	-5.4	-4.3

Ridaforolimus	-10.1	-10.2	-9.7	-9.6	-10.6	-10.7	-9.6	-8.8	-5.3
Selumetinib	-7.2	-7.2	-7.6	-7.7	-7.1	-6.6	-7.4	-5.9	-4.8
Trametinib	-8.2	-9	-7.9	-9.6	-9	-8.6	-8.9	-6.9	-5.5

286

287 In case of PIK3CA, the isoforms PIK3CA-203 & 204 showed low binding affinity with
 288 approved FDA Drugs as these isoforms have short sequences and did not have predicted binding
 289 pocket (Table 3). While the isoforms PIK3CA-201 & 205 showed the best binding affinity with
 290 drugs. Temsirolimus showed good binding affinity with all isoforms

291

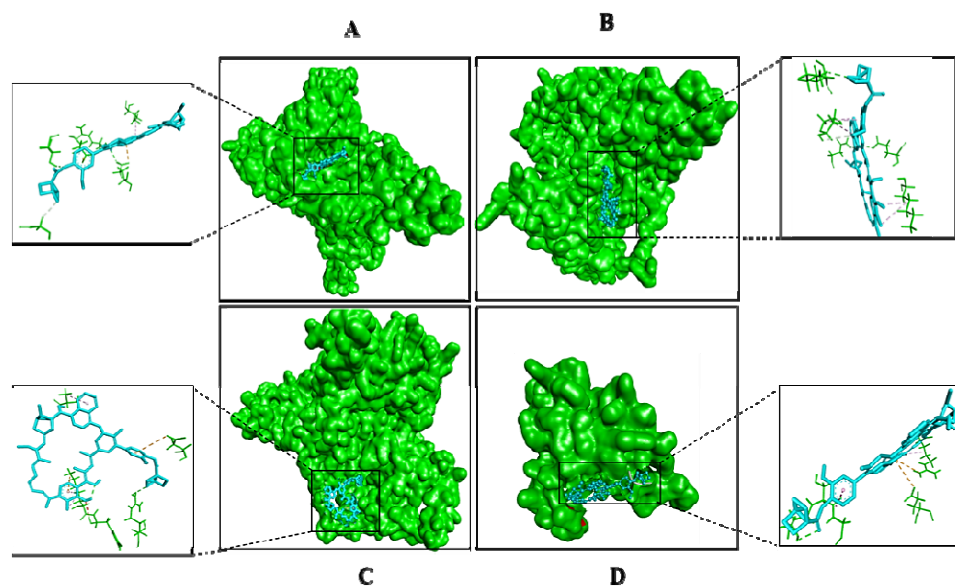
292 **Table 3** Binding affinity values of the PIK3CA-Canonical, PIK3CA-201,205,203 & 204.

Drugs	PIK3CA-Canonical	PIK3CA-201	PIK3CA-205	PIK3CA-203	PIK3CA-204
CC-223	-8.6	-8.3	-8	-6.4	-6.4
ALPELISIB	-8.9	-8.8	-9.5	-7.5	-7.7
BUPARLISIB	-8.6	-8.2	-8.1	-6.2	-6.4
CAPIVASERTIB	-9.5	-9.6	-8.9	-6.6	-6.6
INK-1117	-9	-9	-9	-6.8	-6.8
SERABELISIB	-8.9	-9.1	-9	-6.8	-6.8

TASELISIB	-9.7	-9.7	-8.2	-7.2	-6.9
TEMSIROLIMUS	-9.5	-11.6	-10.2	-9	-9
TRASTUZUMAB	-10.5	-9.6	-9.6	-6.8	-7.7

293

294 To explain how different pocket sizes, shapes, and electrostatic potential surfaces may create the
 295 illusion like the binding mode is different even when the scores are the same in some instances.
 296 Here, we examined Temsirolimus binding mode in all four isoforms and discovered that while
 297 the binding scores are close, the binding patterns vary greatly shown in (Fig. 5). Molecular
 298 docking results of FBXW7, ERBB3 & SMAD4 are shown in supplementary file 4. These results
 299 led us to the hypothesis as, despite the identity of the ligand binding residues, the binding
 300 pocket structures change in size, form, and dynamic properties, resulting in different binding
 301 patterns for a single drug in several isoforms with various binding affinity values.



302

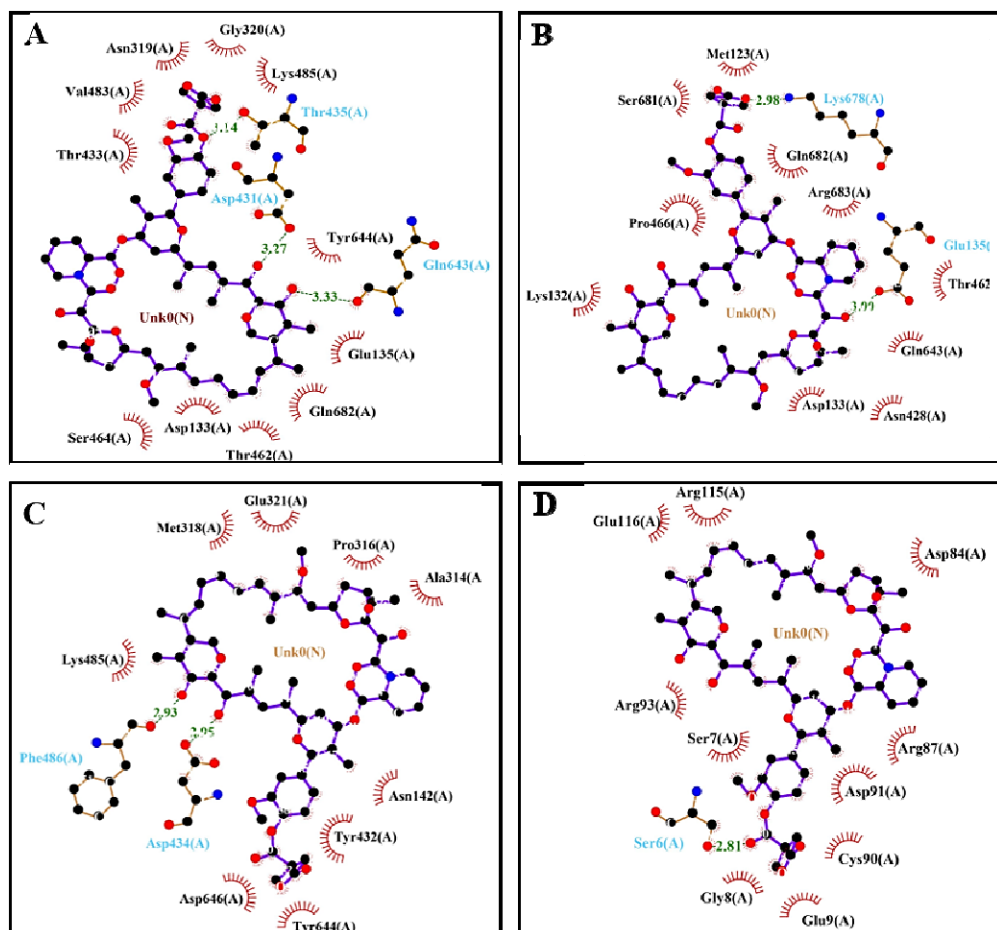
303 **Fig. 5** shows the ligand binding pocket of PIK3CA isoforms A) Canonical Protein B) PIK3CA-
 304 201 C) PIK3CA-205 and D) PIK3CA-202 with the drug Temsirolimus.

305 The interaction analysis of the target proteins isoforms was checked to see what kinds and how
 306 many interactions there were between the docked tesmilorous and the PIK3CA isoforms. When a
 307 complex has a significant number of hydrogen bonds together with a small number of salt
 308 bridges, hydrophobic contacts, and pi-pi interactions, it is said to be strong. To determine how
 309 many interactions each molecule generated, we tested each docked drug differently Fig. 6.
 310 According to the interaction study, complexes with strong binding affinities were those that
 311 produced the most hydrogen bonds (Table 4).

312 **Table.4** Shows the Hydrogen and Hydrophobic interactions of docked isoforms with drugs.

Protein	Hydrogen Interactions	Hydrophobic Interactions
PIK3CA-Canonical	GLU, ASN, ASP, ASP, TYR	THR
PIK3CA-201	ASP, ASN, LYS, SER	LYS, ASP, ASN, PRO, GLN
PIK3CA-205	ARG, ASP, ASP, LYS, PHE	GLU, TYR, LYS
PIK3CA-203	SER,THR	ARG, GLU

313
 314 PIK3CA-Canonical and isoforms 201 & 205 were shown to have strong interactions while the
 315 docked complex of PIK3CA-203 was found to have weak interactions.



316

317 **Fig. 6** Ligplot analysis of interactions between PIK3CA isoforms and Temsirolimus.
 318 Hydrophobic interactions between amino acid residues are shown by red arcs, whereas hydrogen
 319 bonds are represented by green dashed lines with specified bond lengths.

320 4. Discussion

321 Despite the fact that current target prediction methods have shown the accuracy of genomic,
 322 chemical, and pharmacological data in drug target interaction prediction, those methods
 323 frequently only concentrate on the canonical isoforms while disregarding the on- or even off
 324 target isoform-level interactions that are linked to the chemical's action (38). Previous research
 325 has related cancer-specific aberrant splicing to drug resistance mechanisms. However, little is
 326 known about the drug's therapeutic impact on the specified tissue and its side effects on other
 327 tissues. Protein isoforms produced by alternative splicing can express at different levels and
 328 exhibit various, perhaps conflicting, activities in various tissues and/or organs (39, 40), We
 329 postulated in this study that various protein isoforms formed by alternative splicing might

330 develop into candidates for drug interactions that are off-target or non-target because of the
331 presence or lack of target binding sequence in different alternative splicing of genes specifically
332 involved in cervical cancer. Our findings show that most small molecule therapeutic targets have
333 a variety of protein isoforms. As a result, It's therefore feasible which the most of pharmacological
334 targeting genes' protein isoforms have functional differences and show isoform-level changes in
335 its interactions with the drug.

336 As we revealed that KRAS-203 is highly expressed in tumour samples, sequence alignment and
337 data analysis of the gene expression patterns in the TCGA and GTEx datasets uncovered
338 significant data, like medicines that skip alternative isoforms that also expressed in cancer but
339 perhaps are not targeted, while the drugs which might possibly aim alternative isoforms that are
340 variously expressed across many normal tissues, and those are involved in the process of cancer
341 development. Furthermore, the same medication's ability to bind to several structurally related
342 isoforms with various affinities was verified by drug docking study and structural analysis of an
343 example KRAS and PIK3CA protein. These findings basically two processes in which both
344 possibly lead to far-off impacts, which could result in drug resistance.

345 In comparison to the canonical isoform, we observed low expression of KRAS isoforms in
346 TCGA samples. We observed via structural docking research that various medicines can interact
347 with all isoforms in various ways. It is still unknown whether the secondary isoforms behave
348 similarly to or differently from the downregulated primary isoform, carcinogenic, as well as
349 overexpressed. On the other hand, the different isoforms, with the exception of KRAS-204,
350 which was not expressed in normal or tumor samples, showed variable and greater expression in
351 healthy tissue than in tumor tissues. These isoforms can act as tumor suppressors or regulator,
352 counteracting the carcinogenic isoform's function. Immediate inhibition of these isoforms may be
353 undesirable under such conditions. Despite the fact that the precise roles of these isoforms are yet
354 unknown, it's feasible because separating sites from non-targets at the splice level is a crucial
355 step in early stages of drug discovery investigations.

356 Due to restrictions on the availability of data, we were challenged to have several limitations in
357 our current study. The first challenge is the lack of mappings of isoforms between the public
358 online database and older studies. For examples, there is frequently a difference in the exon
359 numbers reported by these two sources. Public databases like Ensemble did not contain many of

360 the isoforms that had previously been described in literature. This makes it extremely
361 challenging to annotate these isoforms structurally and functionally. Therefore, the major aspects
362 of our study are the overexpression of isoforms that are more advantageous for the development
363 of cancer should be suppressed, and the main aims for suppression should be those isoforms that
364 are upregulated in cancer. This is obviously a restriction because these two hypotheses might be
365 incorrect, but as of right now, we don't have any better methods for evaluating the roles of these
366 unidentified isoforms. Furthermore, if there is inclusion of actual protein-level expression of
367 these isoforms will strengthen the claim. As far as we are known, there is currently no
368 comprehensive database that includes the expression of all protein isoforms on a complete
369 proteome scale. In our opinion, the importance of comprehending pharmacological targets at the
370 isoform level should be emphasized even more. However, our results add to those of a recent
371 study that identified means mRNA expression across tissues and variance of expression across
372 tissues as the two key characteristics that separate effective medications from ineffective ones
373 (41).

374 **5. Conclusion**

375 We expect that our findings will encourage more future investigation into the possibility of
376 isoform-level medication design. Enough structural and functional knowledge of these isoforms
377 is necessary to accomplish this aim. Strongly identifying additional cancer biomarkers at the
378 isoform level and connecting them to treatment sensitivity using computational methods would
379 be a crucial next step. If isoform-level drug design is required, accurate structural modelling and
380 prediction of these isoforms are particularly crucial because no database presently has such
381 information about the structure in a well-annotated way. Additionally, various databases should
382 continue to combine isoform-level information and analysis with earlier works of literature and
383 ensure that they are in line, particularly with regard to the functional analyses of less common
384 isoforms.

385

386 **Conflicts of interest**

387 The authors have no conflicts of interest to declare that are relevant to the content of this article

388 **Funding**

389 None

390 **Acknowledgments**

391 I would like to acknowledge the substantial contribution of Muhammad Sajid in providing
392 valuable resources and overseeing the supervision of this project. His guidance and expertise
393 were instrumental in shaping the direction of our work.

394 **References**

395

- 396 1. Yang BH, Bray FI, Parkin DM, Sellors JW, Zhang ZF. Cervical cancer as a priority for prevention in
397 different world regions: an evaluation using years of life lost. *International journal of cancer*.
398 2004;109(3):418-24.
- 399 2. Stuver S, Adami H-O. *Cervical cancer*: Oxford University Press New York; 2002.
- 400 3. Cohen PA, Jhingran A, Oaknin A, Denny L. Cervical cancer. *The Lancet*. 2019;393(10167):169-82.
- 401 4. Crosbie EJ, Einstein MH, Franceschi S, Kitchener HC. Human papillomavirus and cervical cancer.
402 *The Lancet*. 2013;382(9895):889-99.
- 403 5. Small Jr W, Bacon MA, Bajaj A, Chuang LT, Fisher BJ, Harkenrider MM, et al. Cervical cancer: a
404 global health crisis. *Cancer*. 2017;123(13):2404-12.
- 405 6. Howlader N, Ries LA, Stinchcomb DG, Edwards BK. The impact of underreported Veterans Affairs
406 data on national cancer statistics: analysis using population-based SEER registries. *Journal of the*
407 *National Cancer Institute*. 2009;101(7):533-6.
- 408 7. Moore DH. Cervical cancer. *Obstetrics & Gynecology*. 2006;107(5):1152-61.
- 409 8. Kim S, Choi H, Byun J. Overall 5-year survival rate and prognostic factors in patients with stage IB
410 and IIA cervical cancer treated by radical hysterectomy and pelvic lymph node dissection. *International*
411 *Journal of Gynecological Cancer*. 2000;10(4):305-12.
- 412 9. Network CGAR. Integrated genomic and molecular characterization of cervical cancer. *Nature*.
413 2017;543(7645):378.
- 414 10. Oyervides-Muñoz MA, Pérez-Maya AA, Rodríguez-Gutiérrez HF, Gómez-Macias GS, Fajardo-
415 Ramírez OR, Treviño V, et al. Understanding the HPV integration and its progression to cervical cancer.
416 *Infection, Genetics and Evolution*. 2018;61:134-44.
- 417 11. Wilting SM, Steenbergen RD. Molecular events leading to HPV-induced high grade neoplasia.
418 *Papillomavirus Research*. 2016;2:85-8.
- 419 12. Berger AC, Korkut A, Kanchi RS, Hegde AM, Lenoir W, Liu W, et al. A comprehensive pan-cancer
420 molecular study of gynecologic and breast cancers. *Cancer cell*. 2018;33(4):690-705. e9.
- 421 13. Liu S, Zheng B, Sheng Y, Kong Q, Jiang Y, Yang Y, et al. Identification of cancer dysfunctional
422 subpathways by integrating DNA methylation, copy number variation, and gene-expression data.
423 *Frontiers in Genetics*. 2019;10:441.
- 424 14. Pan Q, Shai O, Lee LJ, Frey BJ, Blencowe BJ. Deep surveying of alternative splicing complexity in
425 the human transcriptome by high-throughput sequencing. *Nature genetics*. 2008;40(12):1413-5.
- 426 15. Wang ET, Sandberg R, Luo S, Khrebtkova I, Zhang L, Mayr C, et al. Alternative isoform
427 regulation in human tissue transcriptomes. *Nature*. 2008;456(7221):470-6.

428 16. Keren H, Lev-Maor G, Ast G. Alternative splicing and evolution: diversification, exon definition
429 and function. *Nature Reviews Genetics*. 2010;11(5):345-55.

430 17. Zhang J, Manley JL. Misregulation of pre-mRNA alternative splicing in cancer. *Cancer discovery*.
431 2013;3(11):1228-37.

432 18. Lee SC-W, Abdel-Wahab O. Therapeutic targeting of splicing in cancer. *Nature medicine*.
433 2016;22(9):976-86.

434 19. Climente-González H, Porta-Pardo E, Godzik A, Eyraas E. The functional impact of alternative
435 splicing in cancer. *Cell reports*. 2017;20(9):2215-26.

436 20. Pradella D, Naro C, Sette C, Ghigna C. EMT and stemness: flexible processes tuned by alternative
437 splicing in development and cancer progression. *Molecular cancer*. 2017;16:1-19.

438 21. Safikhani Z, Smirnov P, Thu KL, Silvester J, El-Hachem N, Quevedo R, et al. Gene isoforms as
439 expression-based biomarkers predictive of drug response in vitro. *Nature communications*.
440 2017;8(1):1126.

441 22. Ma J, Wang J, Ghorraie LS, Men X, Chen R, Dai P. Comprehensive expression-based isoform
442 biomarkers predictive of drug responses based on isoform co-expression networks and clinical data.
443 *Genomics*. 2020;112(1):647-58.

444 23. Tate JG, Bamford S, Jubb HC, Sondka Z, Beare DM, Bindal N, et al. COSMIC: the catalogue of
445 somatic mutations in cancer. *Nucleic acids research*. 2019;47(D1):D941-D7.

446 24. Avsec Ž, Agarwal V, Visentin D, Ledsam JR, Grabska-Barwinska A, Taylor KR, et al. Effective gene
447 expression prediction from sequence by integrating long-range interactions. *Nature methods*.
448 2021;18(10):1196-203.

449 25. Freshour SL, Kiwala S, Cotto KC, Coffman AC, McMichael JF, Song JJ, et al. Integration of the
450 Drug–Gene Interaction Database (DGIdb 4.0) with open crowdsourcing efforts. *Nucleic acids research*.
451 2021;49(D1):D1144-D51.

452 26. Wishart DS, Knox C, Guo AC, Shrivastava S, Hassanali M, Stothard P, et al. DrugBank: a
453 comprehensive resource for in silico drug discovery and exploration. *Nucleic acids research*.
454 2006;34(suppl_1):D668-D72.

455 27. Gaulton A, Hersey A, Nowotka M, Bento AP, Chambers J, Mendez D, et al. The ChEMBL database
456 in 2017. *Nucleic acids research*. 2017;45(D1):D945-D54.

457 28. Blum M, Chang H-Y, Chuguransky S, Grego T, Kandasamy S, Mitchell A, et al. The InterPro
458 protein families and domains database: 20 years on. *Nucleic acids research*. 2021;49(D1):D344-D54.

459 29. Goldman MJ, Craft B, Hastie M, Repečka K, McDade F, Kamath A, et al. Visualizing and
460 interpreting cancer genomics data via the Xena platform. *Nature biotechnology*. 2020;38(6):675-8.

461 30. Du Z, Su H, Wang W, Ye L, Wei H, Peng Z, et al. The trRosetta server for fast and accurate protein
462 structure prediction. *Nature protocols*. 2021;16(12):5634-51.

463 31. Kim DE, Chivian D, Baker D. Protein structure prediction and analysis using the Robetta server.
464 *Nucleic acids research*. 2004;32(suppl_2):W526-W31.

465 32. Waterhouse A, Bertoni M, Bienert S, Studer G, Tauriello G, Gumienny R, et al. SWISS-MODEL:
466 homology modelling of protein structures and complexes. *Nucleic acids research*. 2018;46(W1):W296-
467 W303.

468 33. Zhang Y. I-TASSER server for protein 3D structure prediction. *BMC bioinformatics*. 2008;9:1-8.

469 34. Halgren TA. Identifying and characterizing binding sites and assessing druggability. *Journal of*
470 *chemical information and modeling*. 2009;49(2):377-89.

471 35. Mendoza MC, Er EE, Blenis J. The Ras-ERK and PI3K-mTOR pathways: cross-talk and
472 compensation. *Trends in biochemical sciences*. 2011;36(6):320-8.

473 36. Miller S, Tavshanjian B, Oleksy A, Perisic O, Houseman BT, Shokat KM, et al. Shaping
474 development of autophagy inhibitors with the structure of the lipid kinase Vps34. *Science*.
475 2010;327(5973):1638-42.

- 476 37. Goldman M, Craft B, Hastie M, Repěčka K, McDade F, Kamath A, et al. The UCSC Xena platform
477 for public and private cancer genomics data visualization and interpretation. *bioRxiv*. 2019:326470.
478 38. Zhou L, Li Z, Yang J, Tian G, Liu F, Wen H, et al. Revealing drug-target interactions with
479 computational models and algorithms. *Molecules*. 2019;24(9):1714.
480 39. Davuluri RV, Suzuki Y, Sugano S, Plass C, Huang TH-M. The functional consequences of
481 alternative promoter use in mammalian genomes. *Trends in Genetics*. 2008;24(4):167-77.
482 40. Kalsotra A, Cooper TA. Functional consequences of developmentally regulated alternative
483 splicing. *Nature Reviews Genetics*. 2011;12(10):715-29.
484 41. Rouillard AD, Hurlé MR, Agarwal P. Systematic interrogation of diverse Omic data reveals
485 interpretable, robust, and generalizable transcriptomic features of clinically successful therapeutic
486 targets. *PLoS Computational Biology*. 2018;14(5):e1006142.

487

488

489